Inf Syst Front
DOI 10.1007/s10796-009-9149-0

An automated bacterial colony counting and classification system

Wei-Bang Chen · Chengcui Zhang

Abstract Bacterial colony enumeration is an essential tool for many widely used biomedical assays. However, bacterial colony enumerating is a low throughput, time consuming and labor intensive process since there may exist hundreds or thousands of colonies on a Petri dish, and the counting process is usually manually performed by well-trained technicians. In this paper, we introduce a fully automatic yet cost-effective bacterial colony counter which can not only count but also classify colonies. Our proposed method can recognize chromatic and achromatic images and thus can deal with both color and clear medium. In addition, the proposed method is software-centered and can accept general digital camera images as its input. The counting process includes detecting dish/plate regions, identifying colonies, separating aggregated colonies, and reporting colony counts. In order to differentiate colonies of different species, the proposed counter adopts one-class Support Vector Machine (SVM) with Radial Basis Function (RBF) as the classifier. Our proposed counter demonstrates a promising performance in terms of both precision and recall, and is robust and efficient in terms of labor-and time-savings.

Keywords Biomedical image mining · Bacterial colony counting · Segmentation · Clustering · Classification · One-class SVM

W.-B. Chen · C. Zhang (✉)
Department of Computer and Information Sciences,
University of Alabama at Birmingham,
CH 128, 1530 3rd Ave S,
Birmingham, AL 35294, USA
e-mail: zhang@cis.uab.edu

W.-B. Chen
e-mail: wbc0522@cis.uab.edu

Published online: 18 February 2009

1 Introduction

In an oral cavity, there are over five hundred bacterial species and several of them have very close relationship with various dental diseases, such as dental caries and periodontal diseases. Take dental caries as an example, it is reported a most common infectious disease in children and also its prevalence remains on the top of a few diseases in adult. Dental caries is well-known a multi-factor disease. It is not occurred with the absence of either one of fermentable dietary carbohydrate and dental plaque bacteria. To be able to quantify the amount of bacteria in the oral samples, such as saliva samples and plaque samples, is very important for monitoring the progress of the disease and even for indicating the susceptibility of future occurrence of the disease. For periodontal and endodontic diseases, the bacterial culture from the oral samples is also an important diagnostic tool that helps to determine the proper antibiotic agents to use clinically. To analyze the result from bacterial culture, we need to adopt bacterial colony enumeration to count the number of viable bacteria as colonies, and sometimes, there is a need to count the number of colonies of a specific strain.

In general, the diagnostic method is achieved by pouring a liquefied sample containing microbes onto agar plates, incubating the survived microbes as the seeds for growing the number of microbes to form colonies (a.k.a. colony forming unit-CFU) on the plates. The evaluation is done by examining the survival rate of microbes in a sample. These assays are also widely used in biomedical examinations, food and drug safety test, environmental monitoring, and public health (Liu et al. 2004). Figure 1 shows two example images of colonies on a 100 mm Petri dish.

Although this kind of diagnostic assay is very useful, there are two major issues: (1) bacteria colony enumeration,

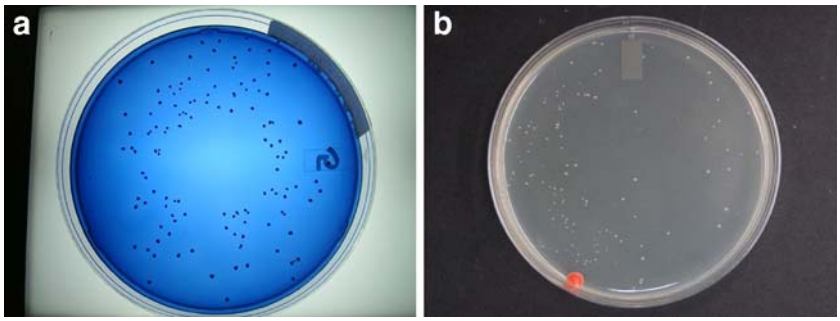

Fig. 1 **a** *Mutans Streptococci* colonies with Mitis-Salivarius agar; **b** *Escherichia Coli* colonies with LB agar, on a 100 mm Petri dish

and (2) bacteria colony classification. The bacterial colony enumerating is a low throughput, time consuming and labor intensive process since there may exist hundreds or thousands of colonies on a Petri dish, and the counting process is usually manually performed by well-trained technicians. The manual counting is an error-prone process since the results tend to have more subjective interpretations and mostly rely on persistent practice, especially when there are a vast number of colonies on the plate (Chang et al. 1994). Thus, having consistent criteria is very important. Another issue is bacteria colony classification. As aforementioned, in an oral cavity, there are over five hundred bacterial species. Hence, it is possible that there is more than one bacteria strain that exists in the sample. Figure 2 shows a Petri dish with several bacteria species from an oral cavity.

In many cases, especially in clinic study, there is often a need to count colonies of a specific strain in a sample. However, to identify a specific strain of colonies is a tough task, even for experienced human operators. To reduce the operator's workload and to provide consistent and accurate results, colony counting devices have been developed and commercialized in the market (Dahle et al. 2004). We review these counters available in the market and classify them into two categories.

The first kind of counter is called automatic digital counters, widely used in most laboratories. However, they are not truly automatic since they rely on technicians who use probe to identify each colony so that the sensor system can sense and register each count.

The second type of counter is semi-automatic or automatic counters. Typically, these counters are often very expensive. These high-priced devices often come with their own image capture hardware for acquiring high quality images to optimize the counter's efficiency and performance. However, the affordability of this kind of equipment is still a non-trivial issue for most laboratories due to the high price of such equipments in the market. Those laboratories that need to perform a huge amount of enumeration tasks may need more than one high-throughput counter to fit their needs. Thus, colony enumeration devices pose a significant budgetary challenge to many laboratories (Putman et al. 2005).

In addition, some automatic counters accurately detect colonies by growing bacteria on special growth medium which contains fluorogenic substrates (COLIFAST 2008). Bacteria metabolize the substrates, and then produce fluorescent product for detection. These systems are extremely sensitive, and are good for detecting micro-colonies. However, the fluorogenic substrates used in the medium are costly, and the fluorescence can only be detected by a sensitive instrument. Besides, some automatic counters (Niyazi et al. 2007) still require users to manually specify the plate/dish area and provide parameters prior to the actual enumeration process. Some may need operators to adjust the threshold values in order to handle dishes/plates/medium that differ from their default settings. In such cases, human operators are heavily involved in the operation, and it is thus not efficient for high throughput processing of plates/dishes. Moreover, most of these automatic counters do not have the ability to identify and enumerate a specific strain from a culture with several bacteria species.

Further, laboratories have needs to use various types of dishes and plates in examinations. However, most of the commercial counters are designed for 60–150 mm Petri

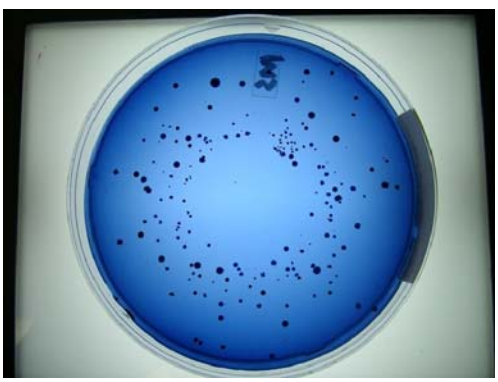

Fig. 2 Bacteria culture contains colonies of different bacteria strains from an oral cavity

dishes, and thus, lack the flexibility for accommodating plates with different sizes and shapes. Furthermore, some existing counters use only binary images for detecting colonies, with which plenty of important properties of the colony, such as color, are lost, which can be used to identify the genus of the bacteria.

To address the above problems, our goal in this study is to design and implement a cost-effective, software-centered system for detecting as well as classifying bacterial colonies in a fully automatic manner. Therefore, more time and money can be allocated to other priorities for those laboratories. Our proposed method can recognize chromatic and achromatic images and thus can deal with both color and clear medium. In addition, as image acquiring devices such as digital cameras and flatbed scanners become popular and affordable, we are motivated to use these devices to obtain cost-effective yet high-quality images for colony counting and classification, without binding to expensive image capturing and display devices. Thus, the proposed method is software-centered and can accept general digital camera images as its input. The counting process includes detecting dish/plate regions, identifying colonies, separating aggregated colonies, and reporting colony counts. In order to differentiate colonies of different species, the proposed counter adopts one-class Support Vector Machine (SVM) with Radial Basis Function (RBF) as the classifier (Schölkopf et al. 1999; Etzion et al. 2005). To our best knowledge, there is no existing commercial tool or software developed by academic researchers that can perform counting and classification at the same time. Our proposed counter has a promising performance in terms of precision and recall, and is efficient as shall be demonstrated in our experiments.

In the remaining of this paper, our preliminary work of this study is described in Section 2. The system details are introduced in Section 3. Section 4 demonstrates the experiment results. Section 5 concludes this paper.

2 Problem statement and initial testing results

In automating the bacteria colony counting process, one of the challenges is to accommodate the variations in the colors of bacteria colony and culture medium. This is because different strains of bacteria may require different nutrients, and these ingredients make the culture medium colored differently. In addition, bacteria that grow on different kinds of culture medium may appear in different color. Hence, while some bacteria colony images contain abundant color/chromatic information, others do not. In general, we can categorize bacteria colony images into two types based on their chromatic features, including chromatic images and achromatic images. For example, Fig. 1a shows the *Mutans Streptococci* grown as black colonies on the blue color Mitis-Salivarius agar. This kind of image is classified as chromatic image since it contains abundant color information. On the contrary, Fig. 1b shows the *Escherichia Coli* grown as white colonies on the clear/transparent LB agar. This kind of image is considered to be achromatic since it lacks color information. Based on our experience with using existing software for colony counting, it is almost impossible for one single system, or a single algorithm, to accommodate the variations in different types of medium. In this study, we intend to process the two types of bacterial colony images that do or do not carry color information in different ways.

Although human operators can easily recognize bacteria colonies on medium after some training, computers can hardly "see" these colonies without any prior knowledge. This motives us to design a three-step approach for simulating human's recognition behavior. When human operators examine a bacteria colony image, they gradually identify objects from the image. First, the dish/plate region, which is the largest object in the image, is identified. Second, within the dish/plate region, one starts to identify colonies based on some criteria such as color and shape. If colonies are clustered together, the operator will try to separate the clustered colonies based on their best visual judgment. In addition, if the dish/plate contains more than one bacteria species, the operator also needs to identify manually the bacteria strain(s) that they are interested. Once all colonies are identified, the operator counts the total number of colonies for each bacteria strain.

The key issues we aim to solve in the first two steps are segmentation and classification problems. Segmentation distinguishes foreground objects from the background, and classification identifies objects of a specific type (e.g., a specific bacteria strain) from a collection of objects. We describe the segmentation problem first, followed by the classification problem since the colony classification is based on the segmentation results.

To identify objects from the background, the edges and contours of objects play an important role in the human visual system. In a chromatic image, we can easily recognize colonies by identifying the color difference between colonies and medium. Hence, we adopt color similarity in HSV (Hue-Saturation-Value) color space to assist the detection of colony boundaries in a chromatic image. On the other hand, we identify colonies in an achromatic image by observing the contrast difference between colonies and medium. An achromatic image can be considered as an intensity (or grayscale) image since it is short of color information. Segmentation in an intensity image is similar to a clustering process which minimizes the intra-class variance of the foreground/background pixels and maximizes the inter-class variance. A brute-

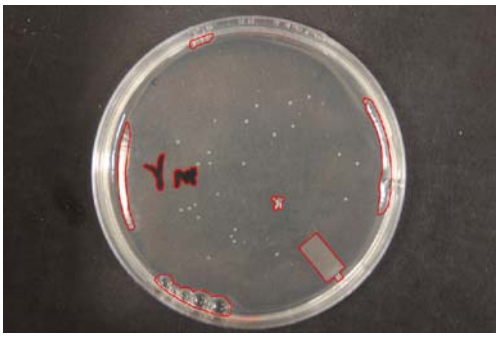

Fig. 3 Artifacts on a 100 mm Petri dish with clear LB agar

force approach can be to use one single threshold to classify pixels into two classes. Otsu's (1979) method is one of the widely used thresholding techniques. It calculates a global threshold for an intensity image and uses it to convert the image into a binary image. However, it is not appropriate to directly use Otsu's (1979) method to extract colony segments due to the following reasons: First, a simple global threshold can cause false positives due to artifacts, such as scratches, dusts, markers, bubbles, reflections, and dents in the image. Figure 3 shows some artifacts on a dish with clear LB agar.

Background intensity variation is another issue because in some cases, especially those with white colonies grown on clear medium, we need to put the dish/plate on a darker surface to enhance the contrast. Otherwise, the colonies cannot be easily seen, even by trained eyes. The background intensity variations can be caused by the different reflecting capabilities of different black surfaces, or sometimes caused by different lighting conditions. In Fig. 4, the top two images show the same Petri dish placed on two different dark surfaces. The image on the right has a much lower intensity (darker) than that of the image on the left. Thus, applying global thresholding techniques directly on those images may result in inconsistent segmentation results due to the variations in background intensities. The bottom two images in Fig. 4 demonstrate the segmentation results by Otsu's (1979) method for the two images in the top row of Fig. 4.

Clustering is another popular choice for object segmentation. To test the performance of clustering techniques on colony images, we applied a commonly used clustering technique, *k*-means clustering, on the bacteria colony images (MacQueen et al. 1967). The *k*-means clustering algorithm initializes k seeds as the centroids of the k clusters. It iteratively assigns each data point to its nearest cluster. Then, the new cluster centroids are calculated for the next iteration. It stops when there is no more data replacement (all clusters are stable). In Fig. 5, the *k*-means clustering results for the two achromatic colony images in Fig. 4 are presented. We choose $k = 3$ in our case, hoping that pixels in an image can be grouped into 3 classes — background, colonies, and artifacts. In Fig. 5, each row corresponds to one of the two images, while each column corresponds to one of the 3 clusters. The non-black pixels represent pixels in the same cluster.

In Fig. 5, we observe that the three clusters roughly correspond to background, colonies, and artifacts, from left to right. However, for the colony cluster (the central column), *k*-means method detects not only the colonies, but also lots of pixels which belong to the medium or dish areas.

The lesson learnt from the above experiments is that it is difficult to use one single thresholding or clustering technique to achieve our goal. In this paper, the proposed framework processes the chromatic and achromatic images

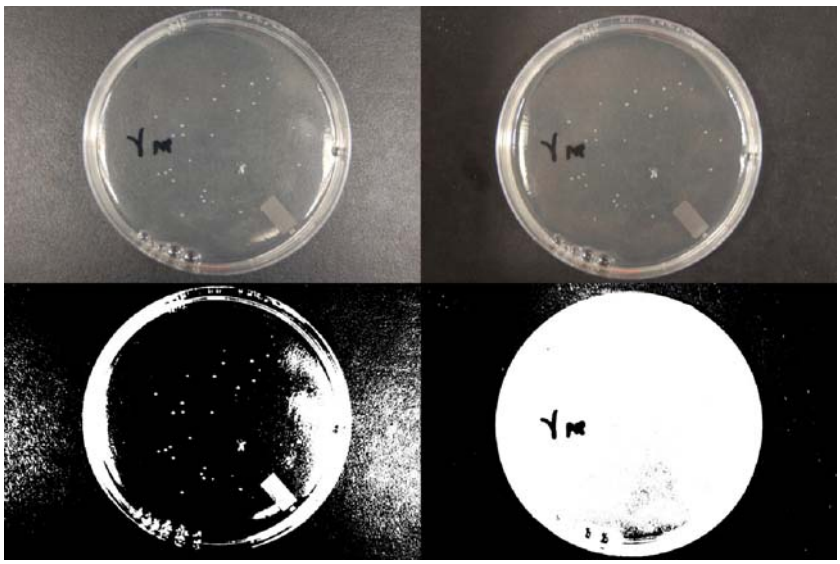

Fig. 4 (Top): The same dish placed on two different black surfaces; (Bottom): The results after applying the Otsu's method directly on the two images at the top

Fig. 5 *k*-means clustering algorithm applied on the two bacteria colony images in Fig. 4

in different ways. In particular, it first determines whether or not an image has color information. Then, the dish/plate area is located. In the third step, colony candidates are identified, which are subject to further statistics test in order to identify the 'true' colonies. Clustered/aggregated colonies are further separated by the use of Watershed algorithm (Luc and Pierre 1991). Finally, we count the surviving colony candidates.

A related yet separate issue is the colony classification. In order to solve this problem, we first extract the features with distinguishing power for each colony, and then develop a classifier based on those features.

To find features which can describe the difference between different types of bacteria strains, we first observe that different types of bacteria will grow as colonies with different morphologies and/or different color/intensity distributions. This is further complicated by the fact that even the same type of bacteria, when grown on different medium, may have different color/intensities. Hence, colony morphology is an important indicator in classifying bacteria strains. In fact, in Holt's book (Holt 1994) titled "Bergey's Manual of Determinative Bacteriology," there are descriptions for the colony morphologies of each bacterial species. Several features, such as size, color, shape, can be used to characterize a colony. We exemplify colonies with different morphologies in Fig. 6.

It is highly possible that two different bacteria strains have similar morphological properties, e.g. in Fig. 6, Columns 1 and 2 are two colonies with different shapes, while their color variances are similar (the color is darker at the center, and relatively lighter at the outer region); Columns 1 and 3 are both round shaped, but their color variances are quite different. Therefore, it is not sufficient to use only one colony feature to distinguish all colonies. In this study, we collect two shape features (solidity, compactness) (Liu et al. 2000) and two color features (first and second order color moments) (Stricker and Dimai 1996), to classify colonies (Huang et al. 1997).

Based on the colony features, we adopt one-class Support Vector Machine (SVM) with Radial Basis Function (RBF) as the core algorithm for colony classification. One-class SVM is a supervised learning method for classification. It is widely used in supervised learning. In this study, we use one-class SVM as the classifier to recognize user specified bacteria strain in the image. With one-class classification, relevant colonies are considered to be alike in a similar way while irrelevant colonies are considered to be outliers that deviate from the target class in their own

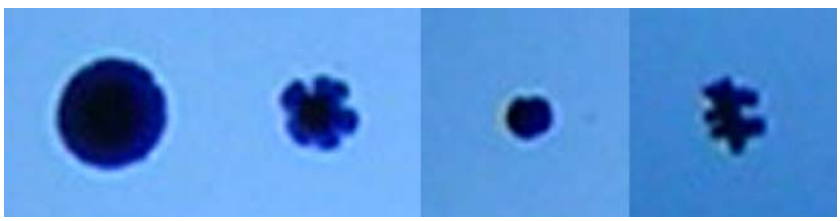

Fig. 6 Bacteria colonies with different morphologies

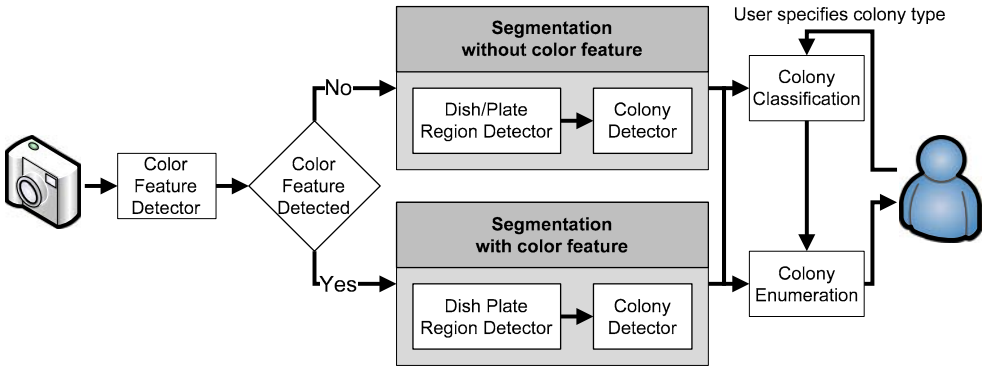

Fig. 7 The overview of the proposed system

ways. The detail of the proposed system is described in Section 3.

3 The proposed system

Figure 7 illustrates the architecture of the proposed system. Given an input image, the proposed system first examines its chromatic/color components, and selects a proper processing method, depending on the type of image (chromatic/achromatic). In the second step, we adopt a fictitious hierarchical structure concept, assuming the image is composed of three layers, including background, container, and colony. These three layers conceptually form a hierarchical structure with three levels since the colonies (top level) are cultured on the dish/plate (middle level) which is encompassed by the background (bottom level). In order to visualize this concept, we compare the bacteria colony image layout to a three-level hierarchical structure in Fig. 8. Based on this hierarchical structure assumption, the proposed system extracts colonies from the image by gradually removing objects from other layers (background and container).

Once all colonies on the image are identified, we check the morphology of each colony object. This is necessary because some colonies may aggregate together to form a larger cluster. Hence, to obtain an accurate colony count, those clustered colonies need to be separated. For this purpose, we adopt the Watershed algorithm to detect and separate those plausible colony clusters. Once all the colony clusters on the dish/plate have been identified and isolated, we simply count the number of detected segments and use it as the total count of bacteria colonies.

For colony classification, at this preliminary stage, we rule out those clustered colonies because Watershed algorithm may sometimes separate a colony with irregular shape (e.g. column 4 in Fig. 6) into a set of smaller colonies. Hence, we perform classification only on those segments considered to be single colony (not clustered). The shape and color features of each single colony are then collected. If the user wants to count the number of colonies of a specific strain, the system prompts the user to select several colony segments of that strain from the image. The selected colonies are used as training data to train a non-linear SVM classifier which classifies all colony segments into two groups — the group of colonies of that specific strain, and all the other colonies (considered outliers to that specific strain) in another group. This allows the system to report the colony count for a particular bacteria strain.

3.1 Color feature detection

As mentioned in Section 2, some bacteria colony images may contain abundant color information. For those chromatic images, we propose a color feature based method to detect foreground objects in the target region (region-of-

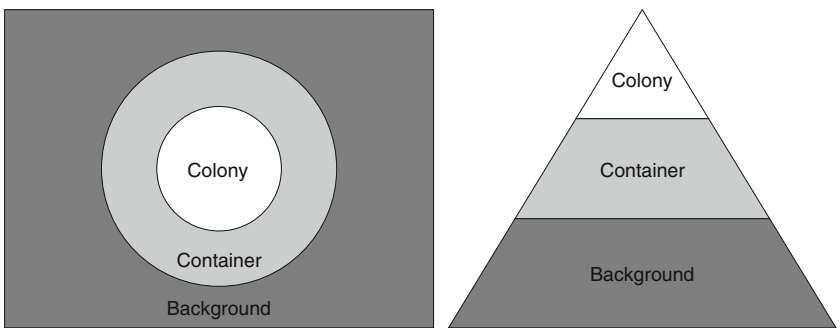

Fig. 8 The hierarchical structure of objects in a bacteria colony image

interest). On the other hand, those images with very little color information (almost no hue) shall be dealt with differently.

To choose a proper segmentation method for each type of image, we first need to determine whether the imported image is chromatic or achromatic. This is achieved by examining the standard deviation of mean values from all three color channels R, G, and B. If the RGB components of a pixel have similar values, it is most likely a gray pixel, and vice versa. Thus, a small standard deviation indicates low hue or a lack of chromatic components. The smaller the standard deviation is, the higher the possibility that the image is achromatic (e.g. those colony images with clear medium and white colonies.) It is at this point that chromatic images (e.g. *Mutans Streptococci* appears as black colonies on the blue color Mitis-Salivarius agar) are differentiated from achromatic images (e.g. *Escherichia Coli* appears as white colonies on the clear LB agar) and they will be dealt with separately. Figure 9 shows two different types of images with their normalized average RGB values (R, G, and B) and standard deviation (S).

In Fig. 9, we show a set of images with different colors and backgrounds. The left column contains dishes with clear LB agar placed on different kinds of black surfaces. The right column contains dishes with blue Mitis-Salivarius agar placed on some bright surfaces. The clear agar forms achromatic images, and the blue agar forms chromatic images. The S (standard deviation) values of the achromatic images are 0.02, 0.01, and 0.04, respectively, and those of the chromatic images are 0.19, 0.19, and 0.14, respectively. This demonstrates that the standard deviation of the average RGB values in an image is an effective indicator of achromatic/chromatic images.

In view of the different characteristics of achromatic and chromatic images, we then develop different segmentation methods for these two types of images in the subsequent image segmentation step.

3.2 Colony segmentation

The core step of the proposed bacterial colony counter is colony segmentation. The goal of segmentation is to distinguish foreground objects from the background. As mentioned earlier in Section 2, global thresholding techniques use a single threshold value to separate foreground from background, while the clustering techniques partition

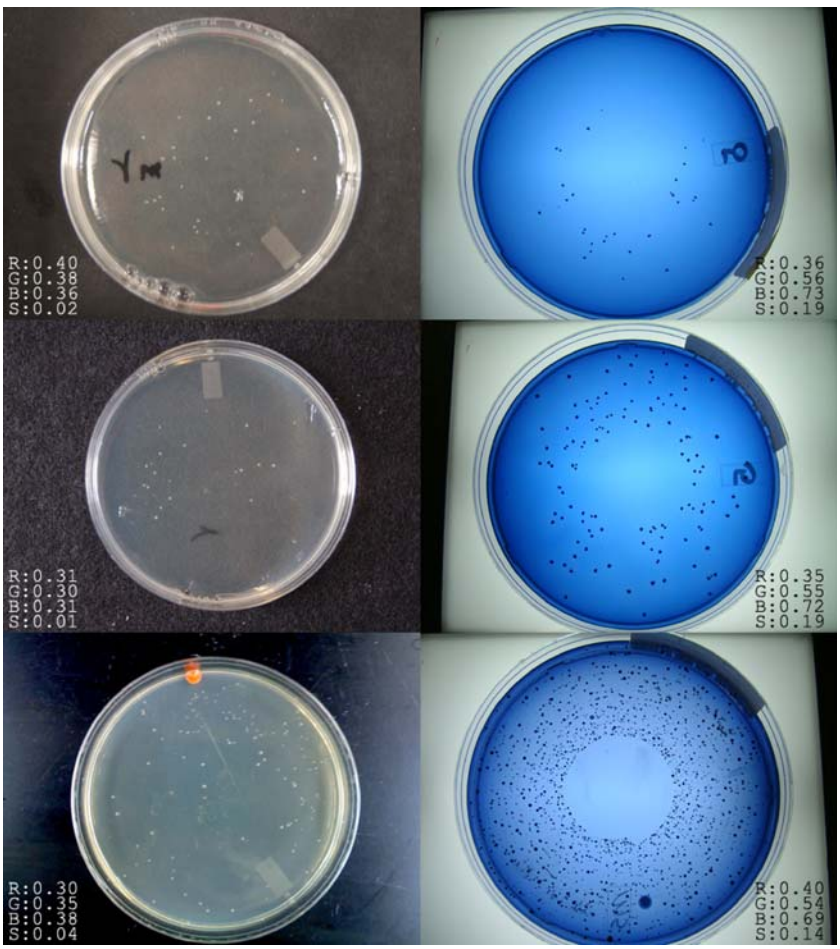

Fig. 9 Differentiating chromatic images (right column) from achromatic images (left column)

objects based on their inter-and intra-class similarities. The thresholding techniques are quite straightforward and efficient, but are not robust when dealing with images containing more than two classes. According to our experiments, the performance of multi-class clustering methods, which are more complicated and usually more time-consuming, is in general worse than that of the thresholding techniques in terms of robustness, explainability, and projectibility. Therefore, in this paper, we propose a thresholding based technique for image segmentation.

To do segmentation with thresholding techniques, we have to solve the problem that the target region contains more than two classes. The natural hierarchical structure of the objects in colony images (as shown in Fig. 8) indicates that we may be able to gradually separate them in a progressive way. Our targeted region, at the first level, is the entire image. The foreground object is thus the dish/plate region, and the background is the area surrounding the dish/plate region. Once the dish/plate area is separated from the background, we proceed to the second level in which the foreground objects become the colonies and the background is the medium and other artifacts in the dish/plate region. With this method, we can gradually isolate small objects from larger ones.

Based on the hierarchical structure aforementioned, the proposed system adopts similar, but slightly different methods in handling chromatic and achromatic images. The major difference lies in whether or not to use the color information in colony segmentation. No matter it is a chromatic or achromatic image, our goal in this step is to identify the dish/plate region in an image, and then, recognize colonies in the detected dish/plate region.

3.2.1 Dish/Plate region detection

The automatic detection of dish/plate regions can relieve the human operators from the tedious work of manually specifying the target dish/plate region. To distinguish the dish/plate region from the background, we first apply the contrast limited adaptive histogram equalization (CLAHE) on the converted grayscale images, which operates on small regions called tiles in the image rather than the entire image (Karel 1994). Each tile's contrast is enhanced and the neighboring tiles are then combined using bilinear interpolation to eliminate artificially induced boundaries.

Then we apply the Otsu's method on the contrast enhanced image to identify the dish/plate region as a target region. For some target regions detected this way, there may be small holes inside, and we fill in the holes by adopting a morphology-based method and consolidate the target regions. Sometimes, this method can also detect some small objects that are not part of the target dish/plate region. We assume the dish/plate region should occupy the most (and central) part of the image, thus there is an extra step in our algorithm which is designed to remove those isolated small objects. Some examples of detected target regions of dish/plate, after applying the above steps, are shown together with their original images in Fig. 10. The results show that the automatic dish/plate region detection algorithm is effective regardless of the size and shape of the dish/plate. After the dish/plate region has been extracted, we can apply segmentation again within the detected dish/plate region.

3.2.2 Colony detection

The second step is to extract colonies from the dish/plate region, and identify single and clustered colonies for subsequent colony enumeration and classification. In order to detect colony segments, in this step, we adopt a color similarity measurement for chromatic images, while using Otsu's thresholding technique on the dish/plate region in achromatic images. For chromatic images, a color similarity metric in HSV (Hue-Saturation-Value) color space (Seber 1984) is adopted for detecting colony boundaries. This is necessary because a simple global threshold cannot extract all colonies due to the existence of artifacts such as scratches, dusts, markers, bubbles, reflections, and dents in the image. The calculation of color similarity in HSV color space is shown in Equation 1.

$$\begin{aligned} CS_{ij} &= 1-\tfrac{1}{\sqrt{5}}\sqrt{(x_j-x_i)^2+(y_j-y_i)^2+(z_j-z_i)^2} \\ x_i &= S_i\times\cos(H_i\times 2\pi) \\ y_i &= S_i\times\sin(H_i\times 2\pi) \\ z_i &= v_i \end{aligned} \tag{1}$$

where CS_{ij} is the color similarity of two pixels i and j. H, S, V are the hue, saturation, and value of a pixel in the HSV color space. This approach is based on the assumption that pixels inside a segment, no matter it is a colony segment or a medium segment, should have higher similarity values with its neighboring pixels than those of the pixels along the segment boundary with their neighbors. We thus calculate the color similarity values between a pixel and its eight neighbors, and use the minimum similarity value to represent the maximum color difference with its neighbors. Thus, pixels inside a segment should have higher minimum similarity values. On the contrary, pixels on the boundary of a segment have lower values. After the calculation, the boundaries are more evident, and the minimum color similarity values form a matrix as a grayscale image as shown in Fig. 11b.

Subsequently, we apply the "Laplacian of Gaussian" (LoG) filter to sharpen the edges. The LoG filter is

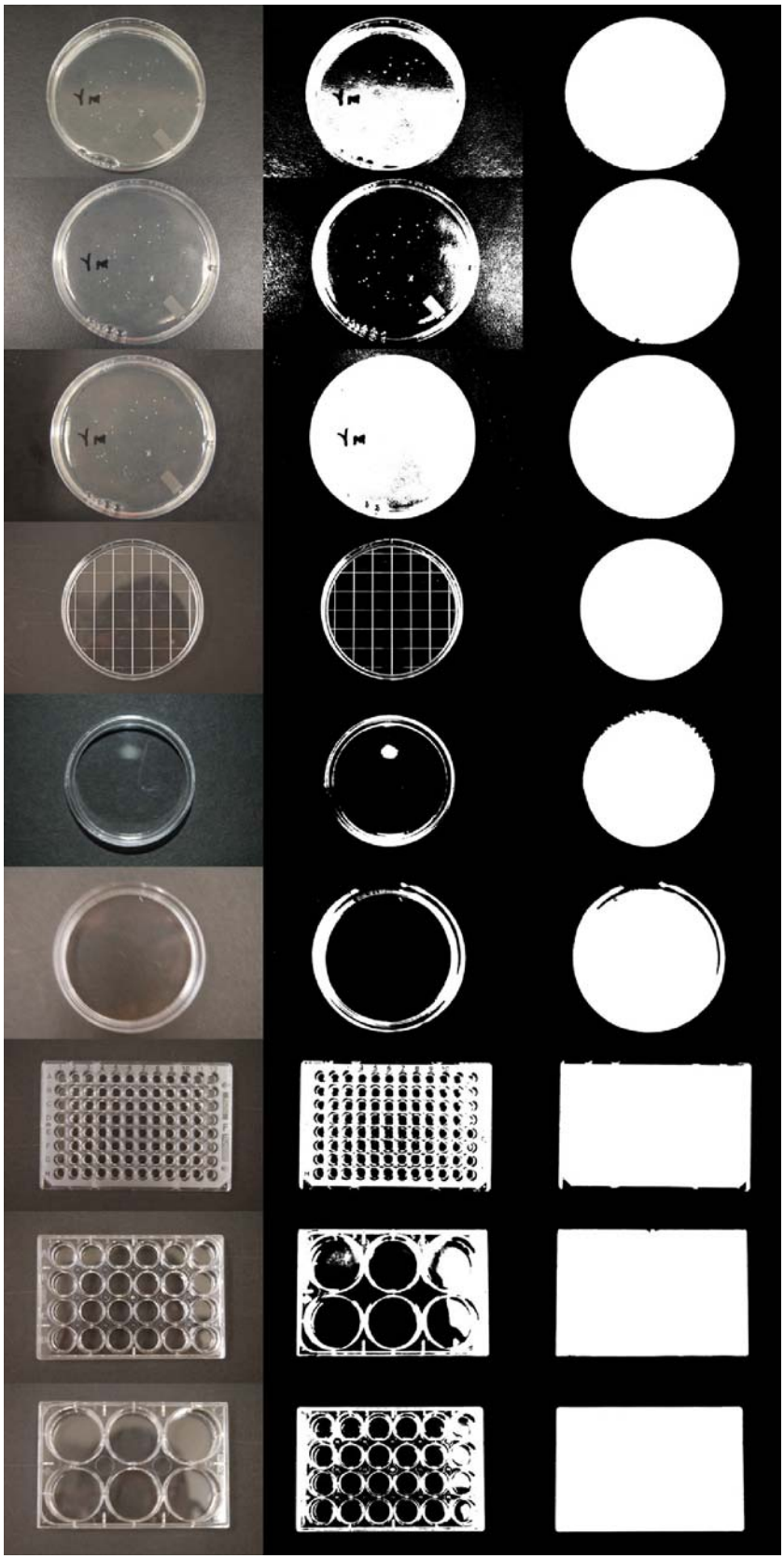

Fig. 10 Segmentation results for detecting dish/plate regions. Raw images (left column); Otsu's method (middle column); the proposed method (right column)

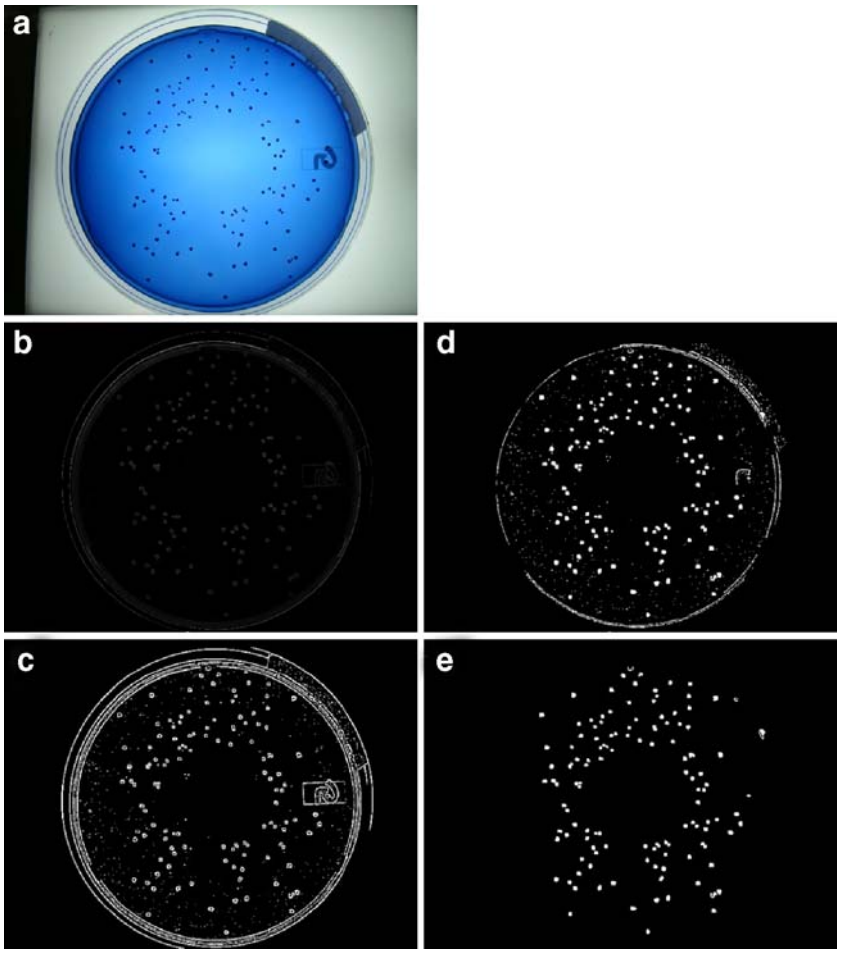

Fig. 11 **a** The raw image; **b** the minimum color similarity image; **c** the result after applying LoG filter; **d** the result after filling closed segments and removing extremely large segments; **e** the result after applying the two-sample Kolmogorov-Smirnov test and a morphological test to remove noise and rim segments

based on the sum of the second derivatives of the two-dimensional Gaussian, which is defined in Equation 2.

$$\mathrm{LoG}_{\sigma}(x,y) = -\left(\frac{x^2+y^2-\sigma^2}{\sigma^4}\right)\cdot e^{-\frac{x^2+y^2}{2\sigma^2}} \quad (2)$$

As shown in Fig. 11c, the edges of segments are sharpened with noise impulse after applying the LoG filter. The image can be considered as a binary image, and the convex hull area of each segment can be examined. If the convex hull area of a segment is extremely large, that segment must be on the rim of the container (or part of the rim). Hence, we can remove those large segments on the rim, and then fill the inner hole of those small segments. To this end, the remaining segments include solid colony segments together with noise segments and few small rim segments. We illustrated the resultant image in Fig. 11d.

For achromatic images, we directly apply the Otsu's method on the dish/plate region in the original achromatic image for colony detection. After this step, colony segments in both types of images are isolated from medium regions. However, there are noise and small rim segments in the background (see Fig. 11d). All these segments are considered to be colony candidates. Next we will examine whether a candidate segment is a noise or rim segment by performing a statistics test and a morphological test, respectively.

3.2.3 Noise removal

The idea of using a statistics test to remove noise segments is based on the assumption that the distribution of pixel values in a colony and that in its surrounding background are significantly different. Hence, we adopt a two-sample Kolmogorov-Smirnov test for this. The two-sample Kolmogorov-Smirnov test compares the distribution of values in the two data vectors x_f and x_b of length n_f and n_b, respectively, representing random samples from some underlying distributions, where x_f are pixel values collected from a segment, and x_b are pixel values collected from surrounding background of that segment. The null hypothesis for this test is that both vectors are drawn from the same distribution, and the alternative hypothesis is that they are drawn from different continuous distributions. The reject of null hypothesis implies the tested segment is a colony. Otherwise, the tested segment is a noise.

However, the tests on rim segments of the dish/plate may reject null hypothesis since they looks quite different from their surrounding backgrounds. To solve this problem, we further examine the location and the morphology of those segments which reject the null hypothesis. This is done on the basis of the observation that a rim segment should be located closely to the boundary of the container, and the variance of its segment width is relatively small.

We estimate the approximate location of a container rim as follow. The radius of a Petri dish is approximated by the minor axis length of the minimum bounding box of the dish region segment. Also, the center of the dish can be detected with Hough transform (Hough 1962). With the dish/plate center and its radius, we can estimate a region that approximately covers the rim of the dish.

The variance of the segment width is evaluated based on their morphology. This is achieved by first rotating the major axis of the minimum bounding box of a segment to x axis, then projecting the width of the segment, i.e. the number of segment pixels along the minor axis, onto the x axis. The projection forms a vector. If the variance of the vector is small, the corresponding segment is more likely to be a rim segment. We illustrate this idea in Fig. 12. We combine the above two criteria to eliminate a segment if it has a small width variance and resides in the rim region. With this method, most of the rim segments can be detected and removed.

3.2.4 Colony separation and enumeration

Ideally, an isolated foreground object from the previous step corresponds to one colony. However, such an object may correspond to more than one colony because several colonies may aggregate together. There is a need to split them in order to get the correct colony counts. The first issue is to distinguish single colonies from clustered colonies. This is done by using the following assumption. In general, the convex hull of a single colony segment is close to a round shape. Thus, its minimum bounding box is close to a square. This implies that the ratio of the major and the minor axis lengths is close to 1. On the contrary, in a clustered colony segment, the ratio of the major and minor axis lengths should be away from 1 since its minimum bounding box is like a rectangle. This property is used in this study to distinguish aggregated colonies from single colonies. In order to split the connected colonies, we consider the intensity gradient image as a topological surfaces (Luc and Pierre 1991), thus the Watershed algorithm can be applied to divide clustered colonies in the image just as water flood in a topographical surface. To illustrate the concept, we demonstrate the application of Watershed algorithm in Fig. 13. After applying the Watershed algorithm, almost all clustered colony segments have been split and are ready for the colony enumeration. After all colonies had been properly split and identified, the final step is to acquire the total number of viable colonies by adding up the number of the segments that have been identified as colonies.

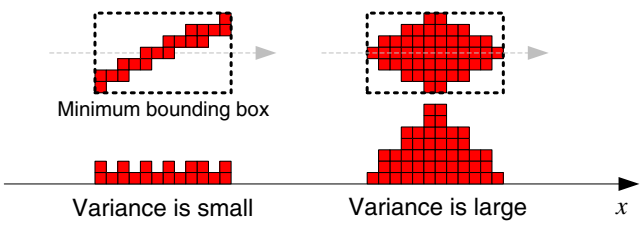

Fig. 12 An example of the segment width variance

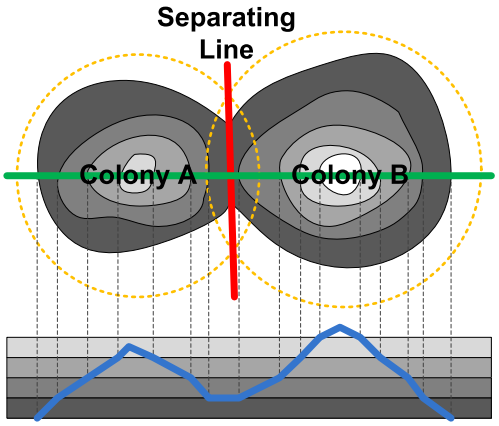

Fig. 13 The concept of Watershed algorithm

3.3 Colony classification

In this paper, we propose to use the one-class Support Vector Machine with Radial Basis Function (RBF) kernel for colony classification. The reason we select a supervised learning method as our classification algorithm is that bacteria colony classification is indeed a complicated task even for well-trained human operators. Therefore, while we always try to minimize the human labor involved, a small effort to help collect the training data is required from the user. This is done via a 'feedback' process in which the user is asked to select 3~9 colonies as the training data for the colony strain that is of his interest.

The one-class SVM can be considered as a hyper-sphere with radius r. The center of this hyper-sphere is the query target, in our case, the user-specified bacteria strain. The one-class SVM collects training data from the user's feedback to construct such a hyper-sphere which encloses colonies of this particular strain. Objects within the hyper-sphere are considered to share common properties, hence classified as one class. All other objects are considered to be outliers of this class.

Before constructing the classifier, our first step is to select the colony feature(s) with the most distinguishing power. In our dataset, we have 4 different bacteria strains as shown in Fig. 6. After carefully examining the data, we extract four features for each colony, including solidity, compactness, color moment 1 (color mean), and color moment 2 (color variance). The solidity feature is defined as the ratio of the segment area to its convex hull area. The compactness feature is defined as the ratio of (segment perimeter)^2 to the segment area. The third feature is color moment 1, which is the mean of the pixel intensity values within the segment. The last colony feature is color moment 2, which represents the variance of the pixel intensity values within the segment.

These four colony features are collected for each single (non-clustered) colony identified in the image segmentation step. The reason we rule out clustered colonies at this stage is that clustered colonies may contain colonies from difference bacteria species. Another reason is that, Watershed algorithm may split those colonies with irregular shape such as the columns 2 and 4 in Fig. 6, although they are not clustered colonies, into a set of smaller colonies. Hence, at this stage of our work towards colony classification, we test our colony classification algorithm only on single colonies at this moment. In addition, we notice that the range of each feature is quite different, and therefore, z-score normalization is performed for each feature before it can be used in the classification.

Our system collects training data from users by prompting them to select several colonies of the specified strain from the given image. The proposed system takes user inputs and retrieves the corresponding features of the selected colonies in the training set. The one-class SVM uses user inputs to construct a classifier, and then applies the classifier on the feature vectors of all the remaining colonies in that image. The classifier will return scores representing the similarity between testing data and the classifier. In general, all data with score value greater than 0 are considered to be in the same class as those in the training set.

4 Experimental results

In our experiments, the test platform is an Intel® Core™ 2 Duo T7700 2.4 GHz machine with 2GB memory. We use four different digital cameras as the image acquiring devices to obtain dish/plate images for bacterial colony detection. The four digital cameras include a Nikon D50 Digital SLR Camera (6.0-megapixel) with a resolution of 3008×2000, a Canon PowerShot A95 Camera (5.0-megapixel) with a resolution of 2592×1944, a Sanyo DSC-J1 Camera (3.2-megapixel) with a resolution 1600×1200, and an Asus P525 PDA cell phone built-in camera (2.0-megapixel) with a resolution of 1600×1200.

Additionally, Petri dishes with two different types of medium and bacteria strains are used in our experiments. The first type of images is obtained from the Department of Pediatric Dentistry at the University of Alabama at Birmingham. This type of plate contains blue color Mitis-Salivarius agar which is used for isolating *Mutans Streptococci*. These acid-producing bacteria attack tooth enamel and cause dental caries. The second type of plate is obtained from the Division of Nephrology, Department of Medicine at the University of Alabama at Birmingham. This type of plates contains the clear LB agar which is widely used in laboratories for *Escherichia Coli* culture.

4.1 Dish/Plate detection

The goal of the dish/plate detection algorithm is to detect the dish/plate area. We compare and evaluate the performance of the proposed dish/plate detection algorithm with Otsu's method by applying both methods on 100 chromatic and achromatic images. Some sample segmentation results are demonstrated in Fig. 10. The performances of both methods are evaluated and compared using the accuracy rate. The accuracy rate is defined as the ratio of the number of accurately detected dish/plate segments to the total number of dish/plate segments, where a dish/plate area is considered accurately segmented if the difference between the detected dish/plate segment and its ground truth mask is less than 5%.

The accuracy rates for the proposed method and Otsu's method are 96% and 38%, respectively. For the 25 chromatic images, the accuracy rates for the proposed method and Otsu's method are 92% and 0%, respectively. For the 75 achromatic images, the accuracy rates for the proposed method and Otsu's method are 97% and 50%, respectively. It is obvious that the proposed method outperforms Otsu's method in dish/plate region detection. We summarize the accuracy rates for both methods in Table 1.

The experimental results show the proposed method outperforms the Otsu's method in processing both chromatic images and achromatic images. It is obvious that using a single thresholding approach alone, i.e. Otsu's

Table 1 Performance comparison for dish/plate region detection

Method	Chromatic images (Amount: 25)	Achromatic images (Amount: 75)	Over all (Amount: 100)
Proposed method	92%	97%	96%
Otsu's method	0%	50%	38%

method, is not sufficient. The reason is that, for chromatic images, the background area and the central part of the dish/plate area are relatively bright due to the light box being used to enhance the contrast. The Otsu's method thus cannot detect the central area of the dish/plate because it has similar intensity as the background. In the case of achromatic images, there are two major factors that make the Otsu's method fail — the uneven medium and the artificial objects such as markers. The former may cause uneven light reflections and cause part of the dish/plate area darker than other areas, while the latter may reduce the brightness of the dish/plate area. On the other hand, the proposed method combines Otsu's method with some morphological constrains and is thus able to recover the missing foreground area and remove the noise from the detected dish/plate area.

4.2 Colony detection

Since the characteristics of the chromatic and achromatic images are quite different, it is more appropriate to discuss the counter performance on them separately. In the experiments, we compared the proposed counter (P.C.) with the Clono-Counter (C.C.) (Niyazi et al. 2007) which is reported by Niyazi in 2007, and the automatic counter (A.C.) proposed in our previous study (Zhang and Chen 2007).

For chromatic images, we test the three counters on 9 images with 2161 colonies in total. The precision values of the A.C. and C.C. methods are 0.97±0.03 and 0.52±0.19, respectively; their recall values are 0.96±0.04 and 0.99± 0.01, respectively; their F-measure values are 0.96±0.01 and 0.67±0.18, respectively. The precision, recall, and F-measure values of the proposed counter (P.C.) are about the same as those of the A.C. method on chromatic images. Table 2 shows the performance comparison on chromatic images.

In addition, the time used by the proposed counter (P.C.), Clono-Counter (C.C), and manual counting (M.C.) is compared. The time used for a counter is greatly affected by the number of colonies in an image, in particular the manual counting. Hence, for a fair comparison, we test these methods on different number of colonies. For manual counting, in general, the ranges in common acceptance for countable numbers of colonies on a 100 mm Petri dish are between 30 and 300 (Breed and Dotterrer. 1916; Tomasiewicz and Peeler 1980). According to this, we select 10 images with colony numbers in this range and then divide them into three groups, including Group I: 30–120 (2 images), Group II: 121–210 colonies (2 images), and Group III: 211–300 colonies (6 images). To avoid bias, we apply each method (including manual counting) to the 10 images for three times. The time used by each method and the output colony counts are also collected for performance comparison.

The experimental results show that for Group I (30–120 colonies), the average running times for P.C., C.C., and M.C. are 27.8±1.0, 44.1±7.5, and 11.0±1.1 (seconds), respectively; for Group II (121–210 colonies), the average running times for P.C., C.C., and M.C. are 27.4±1.1, 39.9± 2.6, and 36.4±3.9 (seconds), respectively; for Group III (211–300 colonies), the average running times for P.C., C.C., and M.C. are 30.8±2.5, 45.9±11.2, and 148.3±14.6 (seconds), respectively. It is obvious that the proposed counter almost always has the shortest time among all three methods, except for Group I in which the number of colonies is small. This is because human counters can easily identify colonies when there are not many, without the need to adopt a complicated segmentation process. However, the manual counting time dramatically increases as the number of colonies is increasing.

In addition to the running time, we also measure the variation of the colony counts for each method. Both C.C. and M.C. methods involve human interventions and may produce various counting results. For Group I, the colony count variations of the P.C., C.C., and M.C. methods are 0.0, 21.6, and 0.8, respectively; for Group II, the variations of the P.C., C.C., and M.C. methods are 0.0, 45.6, and 8.0; for Group III, the variations of the P.C., C.C., and M.C. methods are 0.0, 15.8, and 15.1, respectively. From the above results, we observe that as the number of colonies increases, the variation of the M.C. method also increases. This is because the manual counting is an error-prone process. In the C.C. method, the large variation is due to the different counting areas selected by the human operator.

To evaluate the robustness of the proposed counter (P.C.) on achromatic images, we conduct the following two experiments, and compare the performance of P.C. with that of A.C. and C.C.

In the first experiment, we test the proposed counter (P.C.) on 24 achromatic images (9 good quality images with 1080 colonies and 15 poor quality images with 330 colonies). The performance matrices of the P.C., A.C., and C.C. methods (C.C.[1] in Table 3) on good/poor quality images are summarized in Table 3. From Table 3, we can

Table 2 Performance comparison on chromatic images

Method	Precision	Recall	F-measure
P.C.	0.97±0.03	0.96±0.04	0.96±0.01
A.C.	0.97±0.03	0.96±0.03	0.96±0.01
C.C.	0.52±0.19	0.99±0.01	0.67±0.18

P.C.: The proposed counter

A.C.: Automatic counter (Zhang et al. 2007)

C.C.: Clono-Counter (Niyazi et al. 2007)

Table 3 Performance comparison on achromatic Images

Image Condition	Method	Precision	Recall	F-measure
Good quality (9)	P.C.	0.94±0.07	0.88±0.02	0.90±0.03
	A.C.	0.71±0.06	0.42±0.16	0.52±0.12
	C.C.[1]	0.00±0.00	0.00±0.00	0.00±0.00
	C.C.[2]	0.52±0.13	1.00±0.00	0.67±0.12
Poor quality (15)	P.C.	0.41±0.16	0.98±0.04	0.56±0.13
	A.C.	0.27±0.12	0.84±0.07	0.40±0.12
	C.C.[1]	0.00±0.00	0.00±0.00	0.00±0.00
	C.C.[2]	0.04±0.04	1.00±0.00	0.07±0.07
Overall	P.C.	0.61±0.29	0.94±0.06	0.69±0.20
	A.C.	0.44±0.24	0.68±0.24	0.44±0.13
	C.C.[1]	0.00±0.00	0.00±0.00	0.00±0.00
	C.C.[2]	0.22±0.25	1.00±0.00	0.29±0.31

P.C.: The proposed counter

A.C.: Automatic counter (Zhang et al. 2007)

C.C.[1]: Clono-Counter without preprocessing (Niyazi et al. 2007)

C.C.[2]: Clono-Counter with image preprocessing (Niyazi et al. 2007)

observe that the P.C. significantly outperforms A.C. and C.C. The average overall precision, recall, and F-measure values of the P.C. method are 0.61±0.29, 0.94±0.06, and 0.69±0.20, while the corresponding values of A.C. and C.C. are (0.44±0.24, 0.68±0.24, 0.44±0.13) and (0.00±0.00, 0.00±0.00, 0.00±0.00), respectively. The reason that the C.C. method failed on all achromatic images is that it is designed especially for gray-scale images under the assumption that the foreground intensity is lower than the background intensity. In our data set, however, the achromatic images have bright color foreground objects and dark color background. Hence, the C.C. method cannot be directly applied to our dataset. For a more fair comparison, in the new experiment, we preprocess the achromatic images in order to apply the C.C. method. The preprocessing steps include (1) converting the RGB image into a grayscale image, and (2) inverting the gray-level of the image. After preprocessing, we obtain the overall precision, recall, and F-measure values of the C.C. method (C.C.[2] in Table 3) as 0.22±0.25, 1±0.00, and 0.29±0.31, respectively. The experimental results show that the proposed counter (P.C.) has the highest F-measure value among all the methods.

In the second experiment, we further apply the proposed method on 15 different achromatic images taken from the same dish, but with different background surfaces, zooms, and lighting conditions. We measure the precision, recall, and F-measure of the proposed counter. The average precision, recall, and F-measure on the 15 achromatic images are 0.93±0.11, 0.87±0.04, and 0.90±0.07, respectively. The results of the consistency analysis show the proposed system is quite robust.

4.3 Colony separation

In detecting colonies, there are some clustered colonies that need to be further split into separate colonies. As mentioned earlier, we adopt the Watershed algorithm to solve this problem and find it effective in separating clustered colonies according to our experimental results. An example of the splitting result with the use of Watershed algorithm is given in Fig. 14.

In this experiment, we apply the proposed method on all 8 images that contain clustered colonies. To obtain the ground truth, we visually examined all 115 clustered colony segments carefully and identified in total 240 colonies.

As mentioned earlier in Section 3.2.4, our assumption is that a single colony segment is approximately a round shape such that the ratio of its minor and major axis lengths is close to 1. In other words, the greater deviation the axial

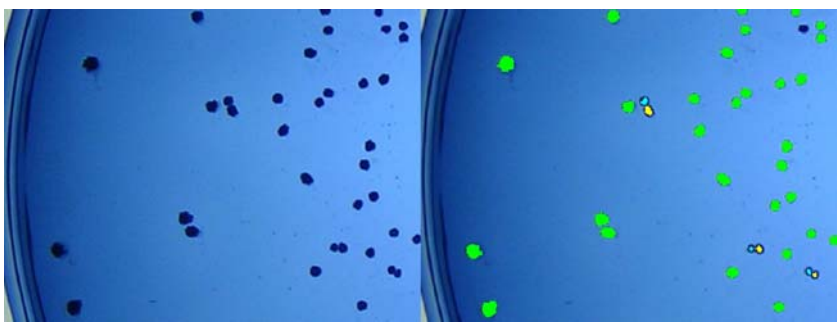

Fig. 14 Clustered colonies separated by the Watershed algorithm

ratio is from 1, the higher the possibility that the segment contains more than one colony. On the basis of this assumption, we set a cutoff value on the ratio (0.7 in our case) in order to obtain the candidate segments for applying Watershed algorithm. Among the 115 clustered colony segments, 101 segments (actually containing 208 colonies) are identified as candidates by our segmentation algorithm. After applying Watershed algorithm on the 101 candidate segments, we successfully identify 167 colonies with no false positives, which is about 80% of the ground truth (208 colonies).

In the proposed system, the colony separation process is an essential step for accurate colony counting. This is especially important when enumerating a large amount of colonies, because high colony density implies more overlapped colonies in a dish/plate. It is worth noting that the Watershed algorithm is an integral part of the proposed system, in which each step contributes to the better performance of the subsequent steps.

4.4 Colony classification

To evaluate the performance of the one-class SVM on bacteria colony strain classification, we apply the proposed classification method on 2 images taken from the same plate, in which there are four different bacteria strains and the morphology of each strain is shown in Fig. 6. The reason for using a single plate in our experiment is that getting the ground truth is very time consuming and labor intensive since we need to manually verify each colony under the golden standard — the microscope. In this plate, the total colony numbers for each bacteria strain are 59, 30, 35, and 20 (S1, S2, S3, and S4 from left to right in Fig. 6), respectively.

In addition, four colony features, including solidity (SO), compactness (CO), color moment 1 (CM1: mean), and color moment 2 (CM2: variance) are collected at the end of the colony detection step. The collected colony features are normalized using the z-score method.

Since one-class SVM is a supervised learning method, users must provide training data to the classifier. In our case, if a user wants to count the colony number of a specific strain, he is required to select several colonies of that strain from the image. The selected colony segments will be used as the training data to construct a one-class SVM classifier. The one-class SVM requires two parameters γ and u as its input, where γ is a variable in the RBF kernel, and u is the percentage of outliers in the whole class. We test on different combinations of $\gamma \in \{0.01, 0.1, 0.5, 1\}$ and $u \in \{0.05, 0.1, 0.2, 0.3, 0.5, 0.7, 0.9, 0.98\}$ in order to find the best parameters. Our experimental results show that the best γ and u values are 0.01 and 0.1, respectively.

While the classification process requires the user to provide training data, the burden put on users should be minimized. To determine the optimal size of the training set, we use S1 which has the most colonies (59 colonies) in the plate, to evaluate how the size of the training set affects the classification results. The size of the training set in our experiment is ranging from 3 to 35 colonies. For each training set size n, we randomly select n colonies from the images as the training set. For each training set, 12 combinations of colony features are tested for training the corresponding one-class SVM classifier. The performance of each classifier is evaluated using the F-measure. To avoid bias, we repeat the above steps 60 times for calculating the average F-measure value for each training set size n and each feature combination.

Since our goal in this study is to enumerate the selected bacteria strain, it is reasonable to emphasize recall more than precision in calculating the F-measure. Figure 15 shows the 4 different weighted F-measures F_2, F_3, F_4, and F_5. For instance, F_2 indicates that recall is twice as important as precision, and F_3 indicates recall is three times as important as precision, and so forth. In each plot, the x-axis is the size of the training set and the y-axis is the corresponding F-measure value. We can observe that as the size of the training set increases, the F-measure value also increases. It is obvious that the F-measure value starts converging when the size of the training set is over 9. Based on the results, both F_4 and F_5 measurements are good enough for performance evaluation. We thus use F_4 measure as the criterion for subsequence performance evaluation.

We can also observe that the F-measure value increases rapidly when the size of the training set changes from 3 to 9. Hence, we use the range of 3 to 9 to evaluate the overall performance of the classification in the subsequent experiments.

The values in Table 4 are obtained by averaging the results for all four types of bacterial colony strains. The experimental results (as shown in Table 4) show that the combination of solidity and color moment 2 (SO+CM2) and the combination of compactness and color moment 2 (CO+CM2) produce the best results (0.915) among all combinations in terms of F_4-measure when the size of the training set is 8. It is worth noting that in our experiments, for each type of strain, the colonies of that strain are randomly divided into two groups, one for training and one for testing. There are in total 60 training-testing groups randomly generated for evaluating the performance of the classifier for each type of strain and each different size of the training set.

Conceptually, the one-class SVM classifier creates a boundary, i.e., a hyperplane, to separate the data points into two groups. In the classification process, the classifier tries to maximize the margin of the hyperplane and minimize the classification error from the training data points. According to this, we may consider adding a feature in the support

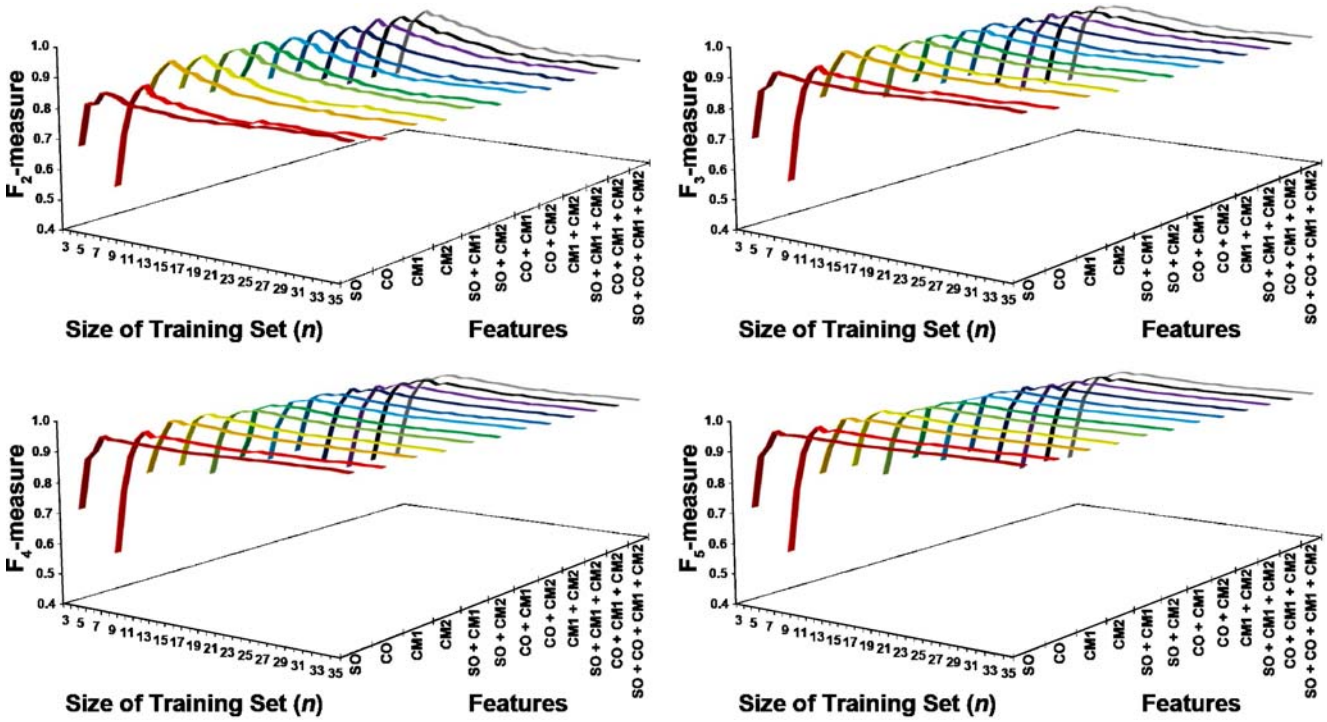

Fig. 15 The classification results for different sizes of the training set

vector as adding a constraint on creating the boundary. Hence, as shown in Table 4, we can observe that the precision value increases while the recall value decreases if more features are used. Although the combination of the four features has the highest precision value, it does not mean this combination is the optimal choice. In fact, the combination of features used to train the classifier should be determined based on the purpose of the applications. For example, the precision value is more important than the recall value in some applications. On the contrary, in some other applications, the recall value is more important than the precision value. For example, recall (a.k.a. sensitivity) is more important in disease screening while precision (a.k.a. specification) is more important in disease differentiation. Thus, it is not recommended to use a single critical value of F-measure for diagnosis. In our case, as aforementioned, since we emphasize recall more than precision, F_4 is used in subsequence performance evaluations.

From Table 4, we observe that the best performance (F_4: 0.915) is achieved when we use 8 training samples and (CO+CM2) or (SO+CM2) features. This setup is thus chosen for the following reasons: 1) First, since one of the goals of the proposed approach is to reduce the manual labor, it is not reasonable to involve too many human interventions, i.e., selecting a large amount of training samples. From that aspect, a small training set is preferred. However, a training set with less than 5 colonies does not have sufficient confidence. According to our experimental results, the average F_4 value, when the training set contains less than 5 samples, is below the acceptable F_4 value of 0.90 for diagnosis. On the other hand, the F_4 values, when the training set has 6~9 examples, are all above 0.90 and converge at around 8 samples. Therefore, we decide to use 8 samples for training the classifier in this paper. 2) Second, in order to select the robust features for classification, we conduct more experiments as shown in Table 5. Table 5 shows the classification performance for each bacterial colony strain when the size of the training set is 8. From the experimental results, we can observe that the feature combinations of (CO+CM2) and (SO+CM2) are quite effective in classifying S1, S2, and S3. For S4, none of the feature combinations really work well. This shows that the combination of color and shape features adopted in this paper do not have sufficient distinguishing power to classify S4 strain, while they are quite sufficient for classifying S1~S3 because of the complementary nature of these two features. Therefore, we decide that the combination of (CO+CM2) or (SO+CM2) is a good compromise between classification accuracy and efficiency, while admitting that more other features that complement the existing combination can be incorporated into the classification step.

5 Conclusions and discussions

The proposed approach (P.C.) is a much improved version of the automatic colony counter (A.C.) developed in our previous study (Zhang and Chen 2007). Like A.C., P.C. is a

Table 4 Colony classification results with different combinations of features and different training data sizes

Size of training set	Feature combination	Overall						Rank
		Precision		Recall		F-measure(F_4)		
		mean	std	mean	std	mean	std	
7	EXP1 (SO)	0.446	0.252	0.977	0.040	0.879	0.064	30
	EXP2 (CO)	0.437	0.234	0.954	0.066	0.853	0.072	54
	EXP3 (CM1)	0.417	0.231	0.987	0.015	0.870	0.097	41
	EXP4 (CM2)	0.472	0.217	0.997	0.007	0.908	0.078	7
	EXP5 (SO+CM1)	0.527	0.290	0.959	0.039	0.876	0.064	34
	EXP6 (SO+CM2)	0.596	0.258	0.969	0.034	0.912	0.053	4
	EXP7 (CO+CM1)	0.508	0.290	0.963	0.041	0.871	0.075	40
	EXP8 (CO+CM2)	0.565	0.254	0.977	0.032	0.913	0.056	3
	EXP9 (CM1+CM2)	0.521	0.262	0.972	0.040	0.893	0.067	15
	EXP10 (SO+CM1+CM2)	0.603	0.289	0.939	0.061	0.881	0.048	27
	EXP11 (CO+CM1+CM2)	0.578	0.288	0.947	0.063	0.882	0.054	26
	EXP12 (SO+CO+CM1+CM2)	0.620	0.296	0.931	0.067	0.877	0.045	32
8	EXP1 (SO)	0.424	0.245	0.989	0.019	0.880	0.079	29
	EXP2 (CO)	0.442	0.257	0.986	0.026	0.876	0.090	35
	EXP3 (CM1)	0.392	0.217	0.995	0.007	0.870	0.103	42
	EXP4 (CM2)	0.437	0.193	0.998	0.004	0.902	0.076	11
	EXP5 (SO+CM1)	0.498	0.282	0.974	0.028	0.880	0.079	28
	EXP6 (SO+CM2)	0.555	0.242	0.980	0.026	0.915	0.055	1
	EXP7 (CO+CM1)	0.487	0.287	0.980	0.022	0.878	0.090	31
	EXP8 (CO+CM2)	0.532	0.248	0.986	0.021	0.915	0.058	1
	EXP9 (CM1+CM2)	0.487	0.241	0.984	0.017	0.897	0.070	13
	EXP10 (SO+CM1+CM2)	0.566	0.282	0.959	0.047	0.891	0.052	20
	EXP11 (CO+CM1+CM2)	0.543	0.278	0.967	0.038	0.893	0.057	16
	EXP12 (SO+CO+CM1+CM2)	0.586	0.293	0.955	0.047	0.892	0.047	19
9	EXP1 (SO)	0.421	0.254	0.992	0.018	0.875	0.095	36
	EXP2 (CO)	0.434	0.255	0.986	0.022	0.871	0.095	39
	EXP3 (CM1)	0.368	0.210	0.995	0.006	0.860	0.107	51
	EXP4 (CM2)	0.413	0.190	0.997	0.004	0.892	0.082	17
	EXP5 (SO+CM1)	0.475	0.280	0.980	0.021	0.874	0.095	37
	EXP6 (SO+CM2)	0.532	0.253	0.988	0.015	0.912	0.074	4
	EXP7 (CO+CM1)	0.461	0.272	0.984	0.016	0.874	0.098	38
	EXP8 (CO+CM2)	0.501	0.243	0.990	0.013	0.909	0.068	6
	EXP9 (CM1+CM2)	0.462	0.237	0.991	0.010	0.895	0.082	14
	EXP10 (SO+CM1+CM2)	0.542	0.289	0.971	0.031	0.891	0.071	21
	EXP11 (CO+CM1+CM2)	0.518	0.276	0.976	0.028	0.892	0.072	18
	EXP12 (SO+CO+CM1+CM2)	0.563	0.304	0.964	0.037	0.889	0.066	22

1. The ranks are produced on the basis of the overall experimental results in which the size of a training set ranges from 3 to 9
2. The experimental results of the training set sizes 3 to 6 are omitted due to the limited space

software-based colony counter which can handle both achromatic and chromatic dish/plate images. The differences between the proposed method (P.C.) and the one in our previous work (A.C.) are: 1) the capability of handling achromatic images has been greatly improved in the P.C. approach. In the P.C. method, we redesign the segmentation algorithm in A.C. for handling both chromatic and achromatic images. In particular, for chromatic images, we apply the "Laplacian of Gaussian" (LoG) filter to sharpen the edges detected by the color similarity method;

for achromatic images, we replace the color similarity method with Otsu's method since there is not much color information in achromatic images. In addition, in order to further reduce the noise, we also propose to use a morphological based approach coupled with a statistics test, i.e., a two-sample Kolmogorov-Smirnov test, in the proposed P.C. method. 2) Another major difference between P.C and A.C. is that the P.C. method has the ability to differentiate between different bacteria colony strains, with little user inputs.

In brief, in this paper, we introduce a robust and effective automatic bacterial colony counter which is capable of recognizing chromatic and achromatic images, detecting dish/plate regions, isolating colonies on the dish/plate, and further, separating the clustered colonies for accurate counting of colonies. In addition, this software-based colony counter has the ability to differentiate between different bacteria colony strains with little user inputs. The proposed counter has the following contributions.

First, our proposed method can handle various kinds of dish/plate images, including round and rectangular shaped dishes/plates. Second, it can accept general digital camera images, which are cost-effective, as its input. In addition, the proposed method can recognize chromatic and achromatic images and handle both color and clear medium. The most challenging part in this study is to handle clear medium images, since colonies look very similar to the background. There also exists a lot of noise on the plate such as bubbles, small scratches, and small markers. Some round-shaped small artifacts also look very similar to the colonies, and sometimes it is hard to tell whether or not they are colonies even by trained human eyes. This makes the colony isolation task extremely difficult. In addition, our system not only can detect colonies on the dish/plate, but also can differentiate colonies of different bacteria species with little user input. The bacteria colony classification is considered a tough task even for a well-trained operator. In this paper, we address those challenges and demonstrate reasonable counting and classification performance for both color and clear medium images.

The above cost-effective features also make our proposed system very flexible and attractive to laboratories. In addition, our counter operates automatically without any human intervention, and the performance is promising, for both color and clear medium. For colony classification, although it still requires some minimal user input, the proposed system demonstrates acceptable results and is much faster than human operators.

Although the performance of the proposed method is promising, we also realize that there still exist several challenges in colony separation as well as colony classification. For example, in colony separation, to determine whether a segment contains clustered colonies is still an

Table 5 Colony classification results with different combinations of colony features

Feature combination	Overall						Bacteria Strains													
							S1			S2			S3			S4				
	Precision (P)		Recall (R)		F_4-measure (F)		P	R	F	P	R	F	P	R	F	P	R	F		
	Mean	std	mean	std	mean	std	mean	mean	mean	mean	mean	mean	mean	mean	mean	mean	mean	mean		Mean
EXP1 (SO)	0.424	±0.245	0.989	±0.019	0.880	±0.079	0.735	0.958	0.939	0.519	0.996	0.945	0.278	1.000	0.867	0.165	1.000	0.768		
EXP2 (CO)	0.442	±0.257	0.986	±0.026	0.876	±0.090	0.711	0.959	0.939	0.637	0.986	0.955	0.272	1.000	0.864	0.149	1.000	0.746		
EXP3(CM1)	0.392	±0.217	0.995	±0.007	0.870	±0.103	0.655	0.986	0.958	0.505	0.994	0.940	0.278	1.000	0.867	0.128	1.000	0.714		
EXP4(CM2)	0.437	±0.193	0.998	±0.004	0.902	±0.076	0.582	0.998	0.958	0.626	0.993	0.959	0.362	1.000	0.906	0.177	1.000	0.785		
EXP5 (SO+CM1)	0.498	±0.282	0.974	±0.028	0.880	±0.079	0.786	0.950	0.938	0.718	0.952	0.934	0.328	0.995	0.888	0.160	1.000	0.761		
EXP6 (SO+CM2)	0.555	±0.242	0.980	±0.026	0.915	±0.055	0.712	0.982	0.960	0.820	0.942	0.934	0.421	0.995	0.921	0.267	1.000	0.846		
EXP7 (CO+CM1)	0.487	±0.287	0.980	±0.022	0.878	±0.090	0.723	0.971	0.951	0.772	0.951	0.938	0.308	0.999	0.882	0.144	1.000	0.741		
EXP8(CO+CM2)	0.532	±0.248	0.986	±0.021	0.915	±0.058	0.647	0.992	0.962	0.839	0.953	0.945	0.409	0.999	0.921	0.235	1.000	0.831		
EXP9 (CM1+CM2)	0.487	±0.241	0.984	±0.017	0.897	±0.070	0.687	0.972	0.949	0.717	0.965	0.946	0.365	0.998	0.906	0.179	1.000	0.788		
EXP10 (SO+CM1+CM2)	0.566	±0.282	0.959	±0.047	0.891	±0.052	0.796	0.943	0.933	0.842	0.902	0.898	0.406	0.989	0.912	0.221	1.000	0.822		
EXP11 (CO+CM1+CM2)	0.543	±0.278	0.967	±0.038	0.893	±0.057	0.739	0.959	0.942	0.839	0.914	0.909	0.396	0.995	0.914	0.197	1.000	0.805		
EXP12 (SO+CO+CM1+CM2)	0.586	±0.293	0.955	±0.047	0.892	±0.047	0.805	0.936	0.927	0.892	0.896	0.896	0.416	0.989	0.915	0.230	1.000	0.829		

issue. In our current approach, the use of the axial ratio of a segment as an indication of clustered colonies is based on the assumption that the clustered colonies are not tightly clustered. However, it is possible that a segment consisting of multiple colonies forms a shape, e.g. triangle or square, with its axial ratio close to 1. As another example, if a dish/plate contains colonies with several different shapes or colonies with irregular shapes, e.g. the right most colonies in Fig. 6, the current approach cannot effectively tell whether a colony segment is an irregularly shaped colony or a clustered colony.

In colony classification, visually identifying bacteria strain is not a trivial task and it has some limitations for the following two reasons. First, sometimes the size of the colony becomes extremely small, i.e. micro-colony, so that we cannot extract their features for classification without using a microscope. Second, bacteria can be grown on several different kinds of culture medium, which may produce colonies with different properties in terms of their color, morphology, etc. Hence, automating the bacteria colony separation and classification process is an important but under-explored field. This paper is our first effort in identifying different strains of bacterial colonies. More efforts will be directed at improving the performance of the bacteria colony classification in our future work. In particular, we plan to detect and distinguish different species of bacteria not only for well-isolated colony, but also for clustered colonies in the dish/plate. The ultimate goal is to accurately classify bacterial colonies according to their strain types and produce the correct count for each class, which could greatly benefit clinical studies.

Acknowledgement This research of Dr. Zhang is supported in part by NSF DBI-0649894 and the UAB ADVANCE program through the sponsorship of the National Science Foundation.

References

Breed, R., & Dotterrer, W. D. (1916). The number of colonies allowable on satisfactory agar plates. *Journal of Bacteriology*, *1*, 321–331.

Chang, C. W., Hwang, Y. H., Grinshpun, S. A., Macher, J. M., & Willeke, K. (1994). Evaluation of counting error due to colony masking in bioaerosol sampling. *Applied and Environmental Microbiology*, *60*, 3732–3738.

COLIFAST, (2008) Retrieved March 3, 2008, from http:// www.colifast.no.

Dahle, J., Kakar, M., Steen, H. B., & Kaalhus, O. (2004). Automated counting of mammalian cell colonies by means of a flat bed scanner and image processing. *Journal of the International Society for Analytical Cytology*, *60*, 182–188.

Etzion, O., Fisher, A., & Wasserkrug, S. (2005). E-CLV: A Modeling Approach for Customer Lifetime Evaluation in e-Commerce Domains, with an Application and Case Study for Online Auction. *Information Systems Frontiers*, *7*(4/5), 421–434.

Hough, P. V. C. (1962). Method and means for recognizing complex patterns. *United States Patent*, *3*, 069–654.

Holt, J. G. (1994). *Bergery's manual of determinative bacteriology* (9th ed.). Baltimore: Williams and Wilkins.

Huang, J., Kuman, S. R., Mitra, M., Zhu, W. J., & Zabih, R. (1997). Image indexing using color correlogram. In *The Proc. of the IEEE International Conference on Computer Vision and Pattern Recognition* (pp. 762–768).

Karel, Z. (1994). Contrast limited adaptive histogram equalization. *Graphics Gems IV: Academic Press Professional*, *Inc*, 447–485.

Liu, W., Wang, T., & Zhang, H. (2000). A Hierarchical characterization scheme for image retrieval. In *Proc. of International Conference on Image Processing*. (pp. 42–45). Vancouver, BC, Canada.

Liu, X., Wang, S., Sendi, L., & Caulfield, M. J. (2004). High-throughput imaging of bacterial colonies grown on filter plates with application to serum bactericidal assays. *Journal of Immunological Methods*, *292*, 187–193.

Luc, V., & Pierre, S. (1991). Watersheds in Digital Spaces: An efficient algorithm based on immersion simulations. *IEEE Transactions on Pattern Analysis and Machine Intelligence*, *13*, 583–598.

MacQueen, J. B. (1967). Some methods for classification and analysis of ultivariate observations, proceedings of 5-th berkeley symposium on mathematical statistics and probability. *Berkeley, University of California Press*, *1*, 281–297.

Niyazi, M., Niyazi, I., & Belka, C. (2007). Counting colonies of clonogenic assays by using densitometric software. *Radiation Oncology*, *2*(4).

Otsu, N. (1979). A threshold selection method from gray-level histograms. *IEEE Transactions on Systems, Man, and Cybernetics*, *9*(1), 62–66.

Putman, M., Burton, R., & Nahm, M. H. (2005). Simplified method to automatically count bacterial colony forming unit. *Journal of Immunological Methods*, *302*, 99–102.

Schölkopf, B., Platt, J. C., Taylor, J. H., Smola, A. J., & Williamson, R. C. (1999). Estimating the support of a high-dimensional distribution. (Technical Report NO. MSR-TR-99–87). Microsoft Research Corporation.

Seber, G. A. F. (1984). *Multivariate observations*. New York: Wiley.

Stricker, M., & Dimai, A. (1996). Color indexing with weak spatial constraints. In *Proc. of SPIE Storage and Retrieval of Still Image and Video Databases IV.* (pp. 29–40). San Jose, CA, USA.

Tomasiewicz, D. M., & Peeler, J. T. (1980). The most suitable number of colonies on plates for counting. *Journal of Food Protection*, *43*(4), 282–286.

Zhang, C., & Chen, W. B. (2007). An effective and robust method for automatic bacterial colony enumeration. In *Proc. of the IEEE International Workshop on Semantic Computing and Multimedia Systems, in Conjunction with the 2007 International Conference on Semantic Computing* (pp. 581–588), Irvine, CA, USA.

Wei-Bang Chen is a Ph.D. candidate in the Computer and Information Sciences Department at UAB. He received a Master's degree in Genetics from National Yang-Ming University in Taipei, Taiwan (1999), and a Master's degree in Computer Sciences from UAB (2005). His main research interests include bioinformatics, multimedia data mining, image processing, and computer vision. His current research involves microarray image and data analysis, biological sequence clustering, biomedical video and image mining, and spam image mining.

Chengcui Zhang is an Assistant Professor of Computer and Information Sciences at the University of Alabama at Birmingham (UAB) since August, 2004. She received her Ph.D. from the School of Computer Science at Florida International University, Miami, FL,

USA in August, 2004. She also received her bachelor and master degrees in Computer Sciences from Zhejiang University in China. Dr. Zhang has authored and co-authored more than 90 research papers in journals, refereed conference/symposium/workshop proceedings, and book chapters focusing in the areas of multimedia databases, multimedia data mining, image and video database retrieval, bio-informatics, and GIS data filtering. She is the recipient of several awards, including the IBM UIMA Award, the UAB ADVANCE Junior Faculty Research Award from the National Science Foundation, UAB Faculty Development Award, and the Presidential Fellowship and the Best Graduate Student Research Award at FIU. She has served in over 100 program committees of major conferences and workshops in multimedia and database systems. Dr. Zhang is serving on the editorial boards for several journals, including International Journal of Multimedia Data Engineering and Management, International Journal of Computer and Informatics, and International Journal of Multimedia and Ubiquitous Engineering, etc. She has also served as a guest editor for IEEE Multimedia Magazine.